Physica B 425 (2013) 23–30

Contents lists available at SciVerse ScienceDirect

Physica B

journal homepage: www.elsevier.com/locate/physb

Effect of vacuum annealing and substrate temperature on structural and optical properties of $ZnIn_2Se_4$ thin films

M.M. El-Nahass, A.A. Attia, G.F. Salem, H.A.M. Ali*, M.I. Ismail

Physics Department, Faculty of Education, Ain Shams University, Roxy, Cairo 11757, Egypt

ARTICLE INFO

Article history:
Received 21 April 2013
Received in revised form
15 May 2013
Accepted 16 May 2013
Available online 29 May 2013

Keywords:
$ZnIn_2Se_4$ films
X-ray diffraction
Annealing
Substrate temperature
Optical properties

ABSTRACT

Zinc indium selenide ($ZnIn_2Se_4$) thin films were prepared by the thermal evaporation technique with high deposition rate. The effect of thermal annealing in vacuum on the crystallinity of the as-deposited films was studied at different temperatures (523, 573 and 623 K). The effect of substrate temperature (623 K) for different thickness values (173, 250, 335 and 346 nm) on the optical parameters of $ZnIn_2Se_4$ was also studied. The structural studies showed nanocrystalline nature of the room temperature (300 K) deposited films with crystallite size of about a few nanometers. The crystallite size increased up to 31 nm with increasing the annealing temperature in vacuum. From the reflection and transmission data, the refractive index n and the extinction coefficient k were estimated for $ZnIn_2Se_4$ thin films and they were found to be independent of film thickness. Analysis of the absorption coefficient data of the as-deposited films revealed the existence of allowed direct and indirect transitions with optical energy gaps of 2.21 eV and 1.71 eV, respectively. These values decreased with increasing annealing temperature. At substrate temperature of 623 K, the direct band gap increased to 2.41 eV whereas the value of indirect band gap remained nearly unchanged. The dispersion analysis showed that the values of the oscillator energy E_o, dispersion energy E_d, dielectric constant at infinite frequency ε_∞, and lattice dielectric constant ε_L were changed appreciably under the effect of annealing and substrate temperature. The covalent nature of structure was studied as a function of the annealing and substrate temperature using an empirical relation for the dispersion energy E_d. Generalized Miller's rule and linear refractive index were used to estimate the nonlinear susceptibility and nonlinear refractive index of the thin films.

1. Introduction

$ZnIn_2Se_4$ (ZIS) is a ternary semiconductor that belongs to $A^{II}B_2^{III}C_4^{VI}$ defect chalcopyrite family. It crystallizes into a structure belonging to the tetragonal space group $I\bar{4}2m$ with lattice parameters $a=5.7095$ Å and $c=11.449$ Å [1]. The crystallite size has been increased initially with increasing annealing temperature [2]. The defect in this compound arises from some percentage vacancies of Zn sites and naturally disorder is created which causes the appearance of a large number of electronic levels in the energy gap both very close to bottom of the conduction band and in the mid gap region [3].

In recent years, increasing attention has been devoted to these compounds [3–17] because of its intrinsic disorder; related properties such as optical and photoconducting [7,8]. Electro-optical memory effect [5] is particularly notable as it is directly related to the defect states which originated due to the intrinsic defects [8]. Photovoltaic devices with the highest conversion efficiency of 15.3% has been reported for Cu(In,Ga)Se_2-based solar cells using ZIS as the buffer layer [18]. Also, electrophotographic layers and devices with high radiation stability have been reported for ZIS [19].

Because of the high density of states near the band edges, the precise determination of the band gap with optical absorption spectroscopy becomes rather difficult and there was contradiction about its nature (direct or indirect) and also different values for it were reported [9]. There is variety in literature about the type of electronic transition and corresponding value of optical energy gap. The optical band gap varied within a very wide range (1.82, 1.95 and 2.6 eV) for ZIS in bulk from [20]. The energy gap of ZIS single crystals was reported to be 1.74 and 1.82 eV with indirect and direct transitions respectively [21]. The analysis of absorption data of ZIS thin films were reported for different techniques employed to grow the layers [12,15–17]. The energy gap of the films grown by the chemical bath method [12] varied in the range, 2.91–3.09 eV with change of precursor concentration. Indirect band gap energy was found to be 1.41 eV for films deposited using a spray pyrolysis technique [15]. The data obtained of films formed by a vacuum deposition process, revealed the existence of allowed direct and indirect transitions with energy gap of 3.38 and 2.22 eV

* Corresponding author. Tel.: +20 1229068680.
E-mail address: hend2061@yahoo.com (H.A.M. Ali).

0921-4526/$ - see front matter © 2013 Elsevier B.V. All rights reserved.
http://dx.doi.org/10.1016/j.physb.2013.05.012

at 300 K respectively [16]. The values of allowed direct and indirect energy gap were found to be 2.3 and 1.76 eV respectively for films deposited using the conventional thermal evaporation technique [17]. These values have been decreased with increasing annealing temperature. Generally, the properties of thin films are highly dependent on the technique used and deposition conditions employed to grow the layers. Therefore, a careful optical absorption study of this compound is required.

Investigations on structural, optical and electrical properties of ZIS films grown by various methods such as chemical transport reaction, chemical vapor deposition with iodine as the transport agent, chemical bath deposition, spray pyrolysis and thermal evaporation have been reported [12–17]. In this paper, the effects of temperature on structural and optical properties of $ZnIn_2Se_4$ thin films prepared by the thermal evaporation technique, with high deposition rate, are reported.

2. Experimental details

Ingots of $ZnIn_2Se_4$ were prepared by fusion of stoichiometric quantities of pure elements in vacuum sealed silica tubes, which were left at 1323 K for 10 h and then cooled to room temperature over 48 h. Thin films of different thicknesses were prepared by the thermal evaporation technique, under a vacuum of about 10^{-4} Pa, with a deposition rate of 20 Å/s. The depositions were made at room temperature onto clean optical flat fused quartz substrates for optical measurements and onto clean glass substrates for structural investigations. The deposited film with thickness of 1254 nm was annealed in vacuum for 2 h at the annealing temperature in the range 523–623 K. Some films deposited at substrate temperature of 623 K with different thicknesses in the range 173–346 nm. The film thickness was monitored during deposition by a quartz thickness monitor. Thickness of deposited films was also checked by the Tolansky's interferometric method [22]. X-ray diffraction (XRD) patterns were obtained for both the powder form and the thin films using a Philips X-ray diffractometer with Cu (k_α) radiation (λ=1.5418 Å).The crystallite size was deduced using the well-known Debye Scherrer formula. The chemical composition was checked by energy dispersive X-ray analysis (EDX). The transmittance T and reflectance R at normal incidence for ZIS films were recorded in the wavelength range 450–2000 nm using a double beam spectrophotometer (JASCO, V-570, UV–visible–NIR). All the measurements were carried out at room temperature. The values of the refractive index n and the extinction coefficient k were computed from the measured T, R and film thickness d by a special computer program using the following equations in case of interference effect is present [23]:

$$T=[(1-R)^2e^{-\alpha d}(1+k^2/n^2)]/[1-R^2e^{-2\alpha d}] \quad (1)$$

where α is the absorption coefficient.

$$R=[(n-1)^2+k^2]/[(n+1)^2+k^2] \quad (2)$$

An approximation can be used in case of semiconductors where $n>k$; $n^2 \gg k^2$. Then Eq. (1) becomes:

$$T=[(1-R)^2e^{-\alpha d}]/[1-R^2e^{-2\alpha d}] \quad (3)$$

Hence α is obtained as

$$\alpha=(1/d)\ln[((1-R)^2/2T)+((1-R)^4/4T^2+R^2)^{1/2}] \quad (4)$$

Then the extinction coefficient k is given by

$$k=\alpha\lambda/4\pi \quad (5)$$

and the refractive index n is given from Eq. (2):

$$n=[(1+R)/(1-R)]+[(4R/(1-R)^2)-k^2]^{1/2} \quad (6)$$

The experimental errors were taken into account to be $\pm 3\%$ for film thickness measurements and $\pm 1\%$ for T and R. The errors in the calculated values of n and k were estimated to be $\pm 3\%$ and $\pm 2.5\%$ respectively. Subsequently the optical parameters were deduced.

3. Results and discussion

3.1. Structural characterization

Fig. 1 shows the energy dispersive X-ray (EDX) spectrum for $ZnIn_2Se_4$ film in as deposited form as a representative example. The XRD pattern of $ZnIn_2Se_4$ in powder form and those of the as deposited (300 K) and annealed films at different temperatures (523, 573 and 623 K) are shown in Fig. 2. The Miller indices (h k l) are indicated on each diffraction peak using (JCPDS-card 80-0424). The XRD pattern of $ZnIn_2Se_4$ in powder form shown in Fig. 2 revealed the polycrystalline nature of the tetragonal structure with lattice parameters a=5.5952 Å and c=11.9886 Å. No other

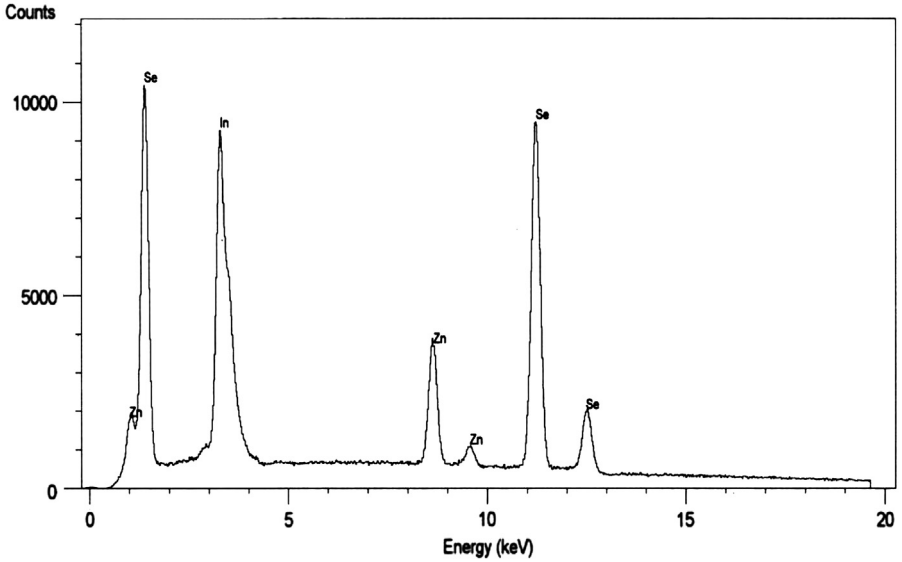

Fig. 1. Energy dispersive X-ray spectrum of $ZnIn_2Se_4$ thin film.

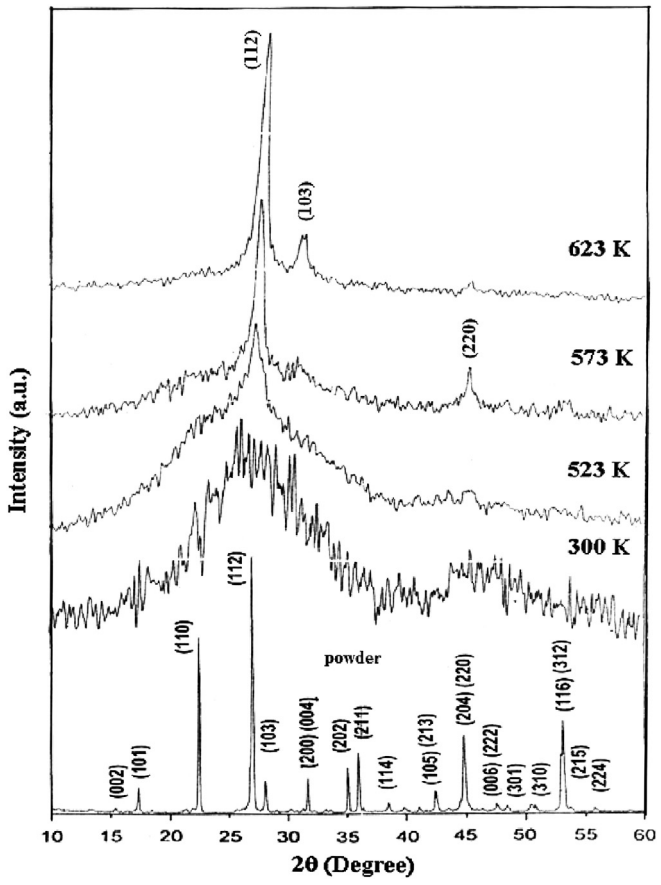

Fig. 2. XRD pattern of $ZnIn_2Se_4$: powder form, as deposited thin film at 300 K, and annealed thin films, of thickness 1254 nm, under vacuum at different temperatures.

observable diffraction peaks corresponding to other binary phases could be detected besides the main $ZnIn_2Se_4$ ternary phase. The polycrystalline structure of the powder form is transformed to nanocrystallite structure by thermal deposition on to glass substrate at room temperature (300 K) with crystallite size of about a few nanometers. A major peak is observed for all annealed samples shown in Fig. 2, at about 26.98° and its equivalent d-spacing is of 3.30 Å which corresponds to reflection from (1 1 2) plane. This indicates that the nanocrystallites are preferentially oriented with (1 1 2) planes parallel to the substrate. The evaluated crystallite size increased appreciably from few nanometers of the as deposited films up to 31 nm with increasing annealing temperature to 623 K. The measurements are performed on (1 1 2) diffraction peak. The formed crystallite size of $ZnIn_2Se_4$ films at different annealing temperatures is calculated from the full width at half maximum, FWHM, of the (1 1 2) peak using Debye–Scherrer's formula [24]

$$D = K\lambda/\beta_o \cos\theta \quad (7)$$

where k is the constant = 0.89, βo is the FWHM, λ is the wavelength of radiation and θ is the angle of diffraction. The obtained results confirmed that the so called intermediate structure between ordered and disordered glassy semiconductor of $ZnIn_2Se_4$ films [25] or so called quasiordered material [26] is a nanocrystallite grain structure $ZnIn_2Se_4$ films [2] and it is not amorphous structure film as it was reported by Refs. [27,28].

3.2. Optical properties

To study the effect of temperature on optical properties of $ZnIn_2Se_4$ thin films, the spectral behavior of the transmittance $T(\lambda)$ and reflectance $R(\lambda)$ are depicted in (Figs.3 and 4). All measurements were performed at normal light incidence in the wavelength range 450–2000 nm. Fig. 3 shows The spectral behavior of $T(\lambda)$ and $R(\lambda)$ for the as deposited film of thickness 1254 nm annealed films in vacuum at different temperatures (523, 573 and 623 K). Fig. 4 shows the spectral behavior of the transmittance $T(\lambda)$ and reflectance $R(\lambda)$ for the deposited films of different thicknesses (173–250–335–346 nm) at substrate temperature of 623 K. It could be noted that all samples show the same character and there is a linear dependence in the region of strong absorption edge. It is also to be noted that the absorption edge is in the wavelength range 500–700 nm separating transparent region from absorption region and can be used to determine the type of optical transition and the corresponding value of energy gap. Above the absorption edge in two Figs. 3 and 4, the appearance of interference maxima and minima at the same wavelength indicating the optical flatness of the deposited films. Fig. 3 revealed that there is influence of annealing temperatures on the transmission edge whereas Fig. 4 revealed that there is no influence of film thickness on spectral behavior of T and R. The values of n and k can be also determined in the same range of wavelength (450–2000 nm). At transparent region of wavelength >1000 nm, $k=0$, and the value of n can only be calculated for such films.

3.2.1. Optical constants

The spectral behavior of the optical constants n and k are depicted in Figs. 5 and 6 respectively for as deposited $ZnIn_2Se_4$ thin film of thickness 1254 nm annealed films in vacuum at different temperatures. Fig. 5. shows that the spectral distribution of refractive index n decreases with increasing annealing temperature. The dispersion curve of refractive index n, for the as deposited films, shows two different intensities peaks at 593 and 670 nm, which can be explained by using multi-oscillator model [29]. The position of these two peaks was slightly shifted to higher wavelength and their intensities decreased as result of annealing. At wavelength >1000 nm, the spectral behavior of n is the normal dispersion, which is explained by single oscillator model [30]. The absorption index k decreases with increasing wavelength and it arrives to zero value at 706 nm for as deposited films at 300 K. This cutoff value of k increases with increasing annealing temperature up to 800 nm at 623 K. After the cutoff values of the absorption index k, an increase of k is observed may be due to the free carrier absorption contribution. The spectral behavior of the optical

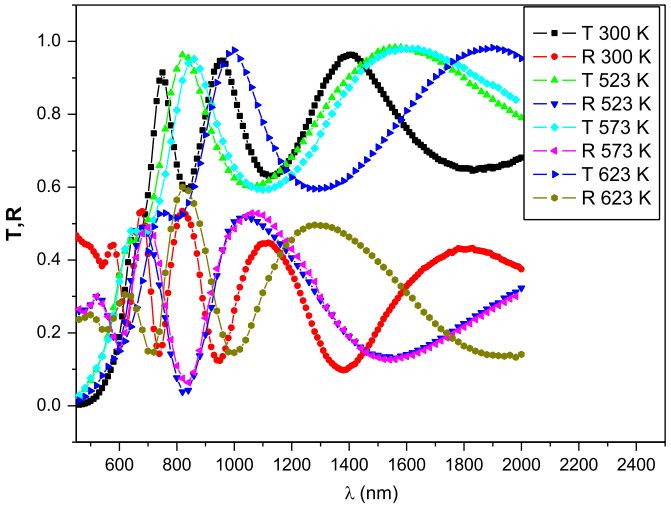

Fig. 3. Spectral behavior of transmittance T and reflectance R for as deposited thin film at 300 K, and annealed thin films of $ZnIn_2Se_4$, of thickness 1254 nm, under vacuum at different temperatures.

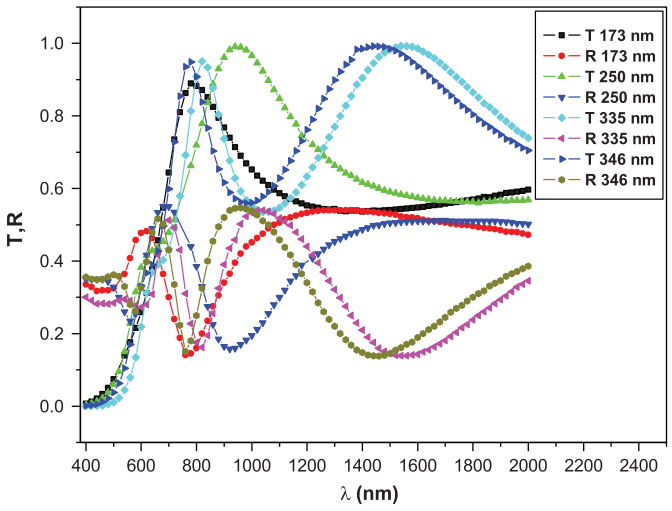

Fig. 4. Spectral behavior of transmittance T and reflectance R for as deposited $ZnIn_2Se_4$ thin films at substrate temperature of 623 K for different thicknesses.

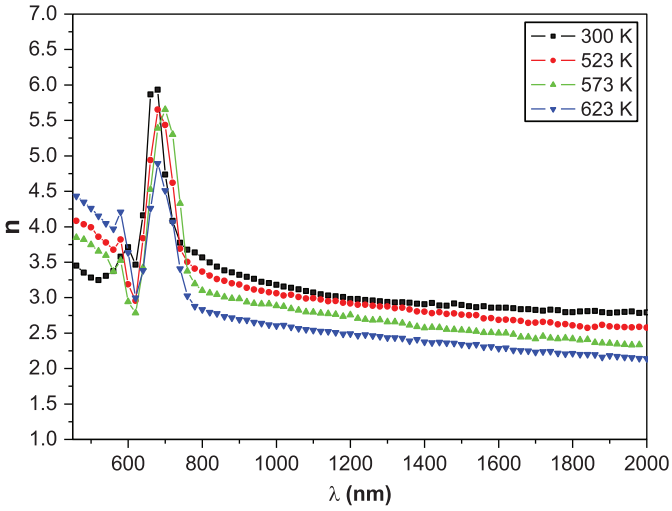

Fig. 5. Spectral behavior of refractive index n of $ZnIn_2Se_4$ thin film, with thickness 1254 nm, for as deposited at 300 K and annealed in vacuum at different temperatures.

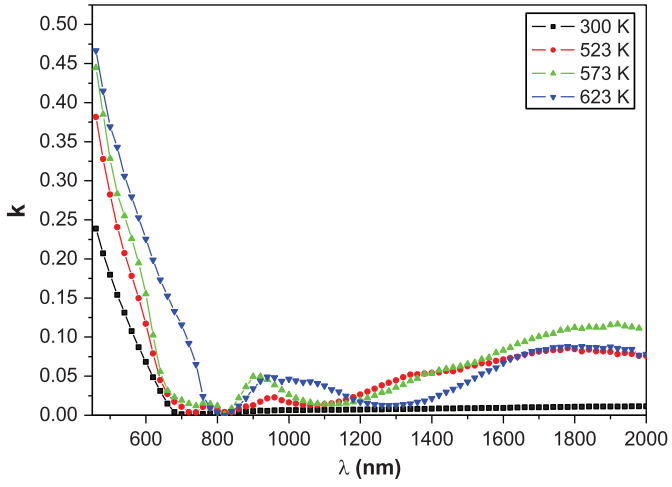

Fig. 6. Spectral behavior of absorption index k of $ZnIn_2Se_4$ thin film, with thickness 1254 nm, for as deposited at 300 K annealed in vacuum at different temperatures.

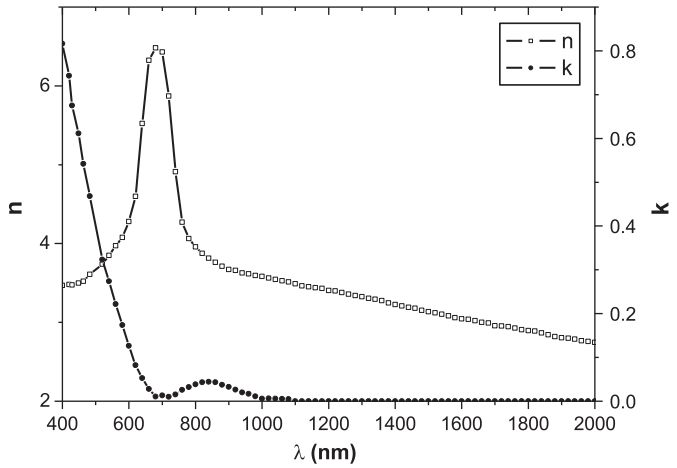

Fig. 7. Spectral behavior of refractive index n and absorption index k for as deposited $ZnIn_2Se_4$ thin films at substrate temperature of 623 K.

constants n and k for $ZnIn_2Se_4$ thin films deposited at substrate temperature of 623 K is depicted in Fig. 7. The results depicted in Fig. 7 represent the average values of n and k for different thicknesses in the range 173–346 nm. The obtained results indicated that the optical constant n and k are independent on the film thickness. One single peak is observed on the dispersion curve of n at 700 nm corresponding to the cutoff value of k as shown in Fig. 7. The behavior of the two curves shown in Fig. 7 is similar to those of the as deposited films at room temperature with increase in both of the intensity of the peak of n at 700 nm and the values of k beginning from 400 nm to the cutoff value of k at 700 nm owing to the effect of substrate temperature. This observation is certainly due to the improvement of crystallinity under the effect of temperature.

3.2.2. Determination of energy gap

The optical energy gap E_g and the type of transition is determined from analysis of the absorption coefficient α near the fundamental absorption edge using the equation by Bardeen et al. [31] as

$$\alpha h\upsilon = A(h\upsilon - E_g)^m \tag{8}$$

where A is a constant depending on the transition probability, h is Planck's constant, υ the incident photon frequency, and $m=1/2$ and $m=2$ for direct and indirect band gap transition respectively. Since $E_g=h\upsilon$, when $(\alpha h\upsilon)=0$, an extrapolation of the linear region of the plots of $(\alpha h\upsilon)^2$ and $(\alpha h\upsilon)^{1/2}$ versus photon energy $(h\upsilon)$ on the x-axis gives the values of the optical band gap E_g. According to the measured absorption spectra, $(\alpha h\upsilon)^{1/2}$ and $(\alpha h\upsilon)^2$ versus $h\upsilon$ curves of $ZnIn_2Se_4$ thin films for as deposited at 300 K and after annealing are shown in Figs. 8 and 9 respectively. Fig. 8 shows an indirect allowed transition with energy gap for as deposited $ZnIn_2Se_4$ thin films of 1.71 eV accompanied with absorption tail of phonon energy of 53 meV. This behavior indicated that the following modified equation represents such a transition.

$$\alpha h\upsilon = B(h\upsilon - E_g^{\text{ind}} \pm E_{\text{phonon}})^2 \tag{9}$$

where E_{ph} is the energy of accompanied phonons. The presence of indirect gaps is attributed to an acceptor-conduction band transition [32]. Fig. 9 illustrates a direct allowed transition with energy gap for as deposited $ZnIn_2Se_4$ thin films of 2.21 eV. Such a transition occurs in case that the incident photon energy is higher than 2.21 eV. The values of energy gap of as deposited $ZnIn_2Se_4$ thin films grown by different techniques and the values obtained in the present work were listed in Table 1. The band gap values obtained in this work of as deposited films are in good agreement

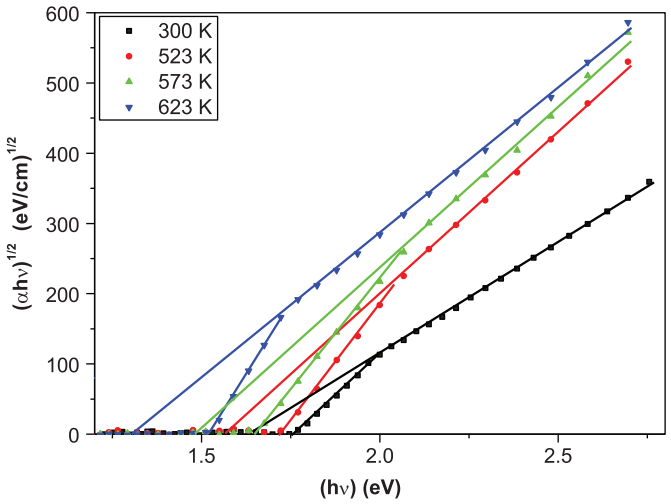

Fig. 8. Dependence of $(\alpha h\nu)^{1/2}$ on $(h\nu)$ of $ZnIn_2Se_4$ thin films for as deposited annealed in vacuum at different temperatures with thickness 1254 nm.

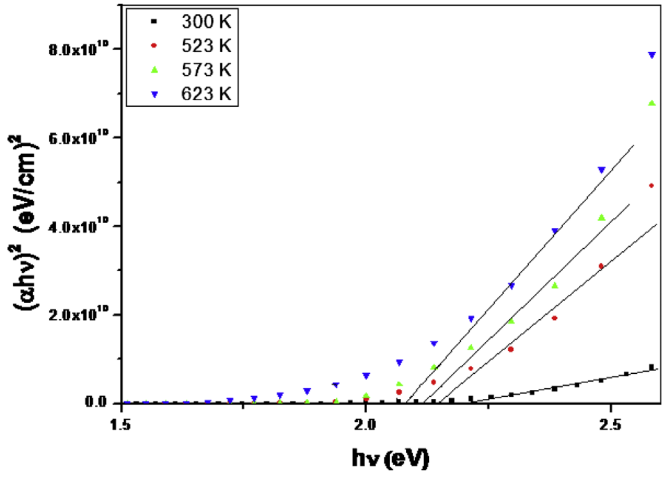

Fig. 9. Dependence of $(\alpha h\nu)^2$ on $(h\nu)$ of $ZnIn_2Se_4$ thin film, with thickness 1254 nm, for as deposited at 300 K and annealed in vacuum at different temperatures.

Table 1
The values of energy gap of as deposited $ZnIn_2Se_4$ thin films grown by different techniques compared with the values obtained in the present work.

Transition type	E_g (eV) [16]	E_g (eV) [15]	E_g(eV) [17]	E_g (eV) [12]	E_g (eV) (present study)
Direct allowed	3.38	–	2.3	2.91–3.09	2.21
Indirect allowed	2.22	1.41	1.76	–	1.71

with the values reported by Zeyada et al. [17]. The other values of the energy gap listed in Table 1 are not in agreement with this work and this can be attributed to the deposition technique and deviation of the material from the stoichiometry. The values of indirect and direct energy gap for as deposited $ZnIn_2Se_4$ thin films decreases with increasing annealing temperature as shown in (Figs. 8 and 9) and also in Table 2. Fig. 10 shows the variation of both direct E_g^d and indirect E_g^{in} optical band gaps of $ZnIn_2Se_4$ thin films versus annealing temperature. It is clear from this data that the increase of annealing temperature leads to the increase in the crystalline part as shown in Fig. 2 and decrease in the absorption edge as shown in Fig. 3 and thus decrease in the values of direct and indirect optical band gaps. This behavior is in agreement with that reported by Hendia and Soliman [33]. Figs. 11 and 12 show the plot of both $(\alpha h\nu)^{1/2}$ and $(\alpha h\nu)^2$ versus $h\nu$ for $ZnIn_2Se_4$ thin films deposited at substrate temperature of 623 K. The results illustrate an indirect and direct allowed transition with energy gaps of 1.70 eV and 2.41 eV respectively. The value of the energy of accompanied phonon is of 44 meV for $ZnIn_2Se_4$ thin films deposited at substrate temperature of 623 K. The variation in direct and indirect energy gaps of $ZnIn_2Se_4$ thin films as a function of temperature is indicated in Table 2. The optical energy gaps obtained in this work is in agreement with the values reported by some authors [2,15,21,34–36], but differ from the results obtained by some others [12,27,33].

3.2.3. Dispersion analysis

In order to analyze the refractive index dispersion of the films, we used the single-oscillator model, developed by Wemple and DiDomenico [30]. The single-oscillator model for the refractive index dispersion can be expressed as follows [30]:

$$n^2 = 1 + [E_d E_o / E_o^2 - (h\nu)^2] \quad (10)$$

where E_o is the single-oscillator energy for electronic transitions and E_d is the dispersion energy which is a measure of the strength of inter band optical transitions. E_o and E_d can be obtained from Eq. (10) by Plotting $(n^2-1)^{-1}$ versus $(h\nu)^2$ as shown in Figs.13 and 14. Fig. 13 illustrates the plot of $(n^2-1)^{-1}$ versus $(h\nu)^2$ for $ZnIn_2Se_4$ thin films of thickness 1254 nm deposited at 300 K and annealed in vacuum at different temperatures (523, 573 and 623 K). Fig. 14 shows the plot of $(n^2-1)^{-1}$ versus $(h\nu)^2$ for as deposited $ZnIn_2Se_4$ thin films at substrate temperature of 623 K with thickness range 173–346 nm. The values of E_o and E_d are directly determined from the intersection with the vertical axis (E_o/E_d) and the slope $(E_oE_d)^{-1}$. The calculated values of E_o, E_d and the corresponding dielectric constant at infinite frequency ε_∞, are tabulated in Table 2.

In the transparent region, the relation between the refractive index n and the wavelength λ is given by the following relation [37]:

$$n^2 = \varepsilon_L - (e^2/4\pi^2 C^2 \varepsilon_o)(N/m^*)\lambda^2 \quad (11)$$

where ε_L is the lattice dielectric constant, c is the speed of light, ε_o is the permittivity of free space and N/m^* is the ratio of carrier concentration to the effective mass. The values of ε_L and N/m^* can be obtained by plotting n^2 versus λ^2 as shown in Figs. 15 and 16. These two figures illustrate the plot of n^2 versus λ^2 for $ZnIn_2Se_4$ thin films deposited at 300 K and annealed in vacuum at different temperatures and films deposited at substrate temperature of 623 K respectively. These figures also show that n^2 decreases nonlinearly with increasing λ^2. The value of ε_L is determined from the extrapolation of the linear portion of the curve towards $\lambda^2=0$ and its slope results in the value of N/m^*. The values of ε_L and N/m^* are also listed in Table 2. The disagreement between values of ε_∞ and ε_L indicates formation of free carriers in $ZnIn_2Se_4$ thin films [38].

Empirical relation for the dispersion energy E_d is given by [30]

$$E_d = \beta N_c Z_a N_e \quad (12)$$

where β has a value of 0.37 ± 0.05 eV for the covalent compounds, $N_c=4$ is the cation coordination number, $Z_a=2$ is the formal chemical valence of the anion and $N_e=8$ is the average number of valence electrons per anion. The covalent nature of structure tends to decrease with increasing annealing temperatures, which corresponds to decrease of β values shown in Table 2. Furthermore, the value of β is increased at substrate of temperature of 623 K. The values of β are somewhat different from the

Table 2
Temperature dependence of optical parameters of $ZnIn_2Se_4$ thin films.

Annealing temperatures (K)	E_o (eV)	E_d (eV)	n_o	$\chi^{(3)}$ (10^{-11}esu)	n_2 (10^{-10}esu)	E_g (eV)		ε_∞	ε_L	β (eV)	N/m^* (10^{56} kg^{-1} m^{-3})
						direct	indirect				
(3 0 0)*	2.29	16.19	2.84	1.70	2.26	2.21	1.71	8.08	10.18	0.25	8.02
(6 2 3)**	2.08	16.52	2.99	2.71	3.42	2.41	1.70	8.95	12.83	0.26	16.80
523	2.41	14.83	2.67	0.98	1.38	2.16	1.64	7.15	9.21	0.23	8.32
573	2.44	12.83	2.50	0.52	0.79	2.13	1.56	6.25	7.98	0.20	8.11
623	2.46	10.58	2.30	0.23	0.38	2.08	1.41	5.30	6.80	0.17	6.92

* as deposited temperature.
** substrate temperature.

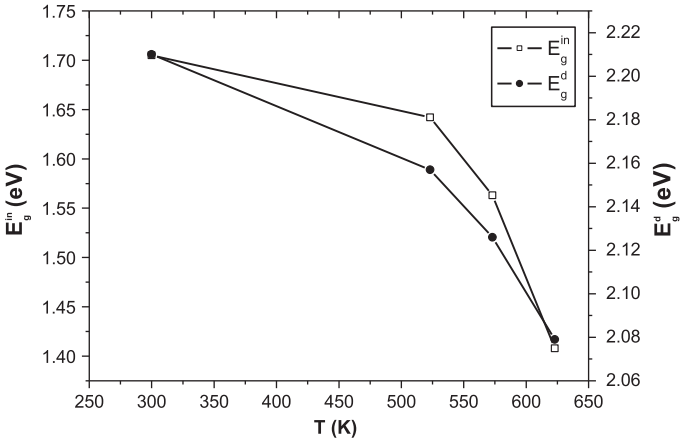

Fig. 10. Variation of both direct E_g^d and indirect E_g^{in} optical band gaps of $ZnIn_2Se_4$ thin films versus annealing temperature.

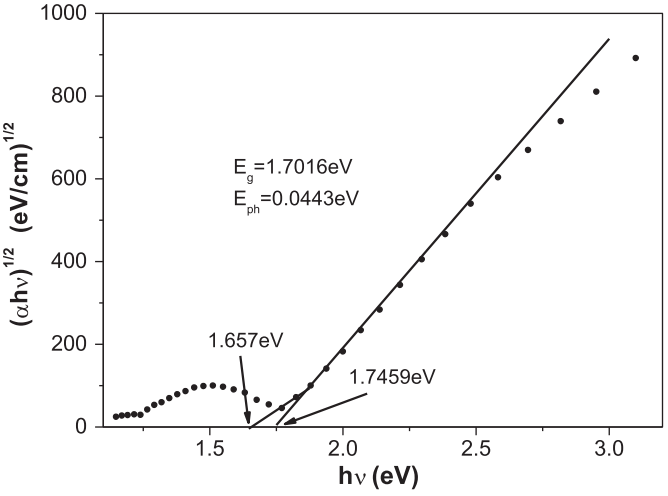

Fig. 11. Dependence of $(\alpha h\nu)^{1/2}$ on $(h\nu)$ for as deposited $ZnIn_2Se_4$ thin films at substrate temperature of 623 K.

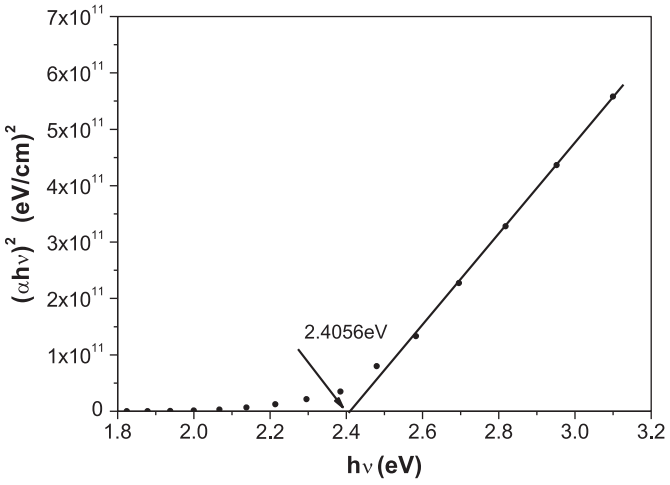

Fig. 12. Dependence of $(\alpha h\nu)^2$ on $(h\nu)$ for as deposited $ZnIn_2Se_4$ thin films at substrate temperature of 623 K.

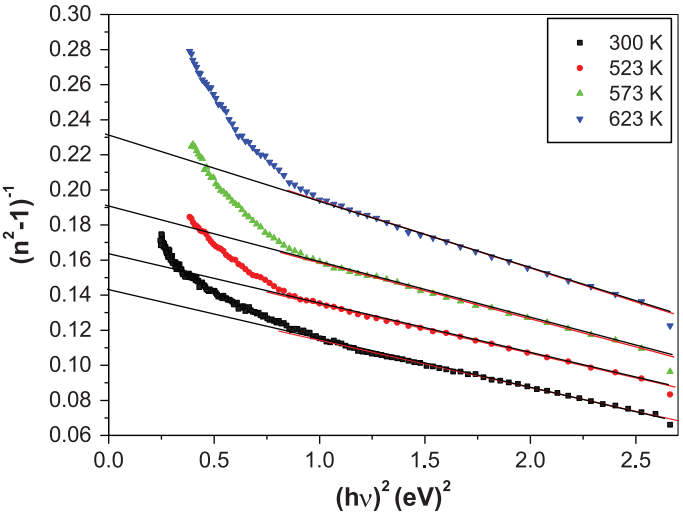

Fig. 13. Plot of $1/(n^2-1)$ versus $(h\nu)^2$ of $ZnIn_2Se_4$ thin films, with thickness 1254 nm, for as deposited at 300 K and annealed in vacuum at different temperatures.

reported one for the covalent compounds, that can be attributed to the deviation of films from stoichiometry and also may be due to the defect chalcopyrite structure of $ZnIn_2Se_4$.

Semi-empirical relation based on Miller's generalized rule [39] can be used for the estimation of the nonlinear refractive index n_2 and susceptibility $\chi^{(3)}$. A combination of Miller's generalized rule with linear refractive index and WDD dispersion parameters E_o and E_d are used to calculate the nonlinear susceptibility $\chi^{(3)}$ by the following relation [40]:

$$\chi^{(3)} = A_o(E_d/E_o)^4/(4\pi)^4 = A_o(n_o^2-1)^4/(4\pi)^4 \quad (13)$$

where Ao is 1.7×10^{-10} (for $\chi^{(3)}$ in esu) and n_o is the static refractive index calculated using Eq. (10) at the limit of n as $h\nu$ approaches zero, $n_o=(1+E_d/E_o)^{1/2}$; $\varepsilon_\infty = n_0^2$.

The n_2 can be calculated from the relation [41]

$$n^2 = 12\pi\chi^{(3)}/n_o \quad (14)$$

The static refractive index n_o, susceptibility $\chi^{(3)}$ and nonlinear refractive index n_2 are tabulated in Table 2.

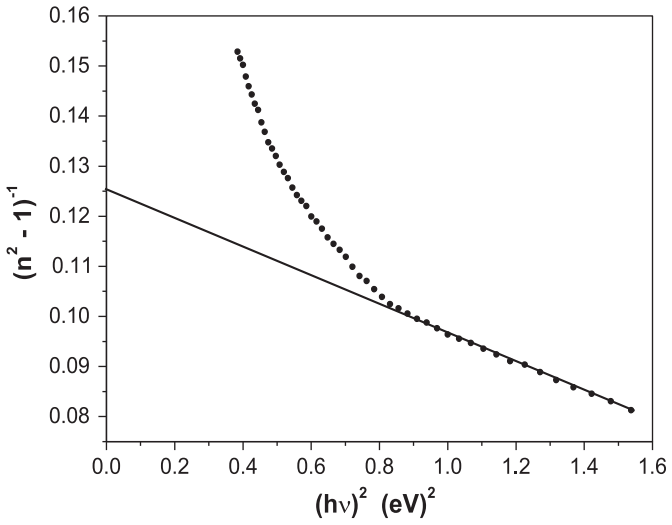

Fig. 14. Plot of $1/(n^2-1)$ versus $(h\nu)^2$ for as deposited $ZnIn_2Se_4$ thin films at substrate temperature of 623 K.

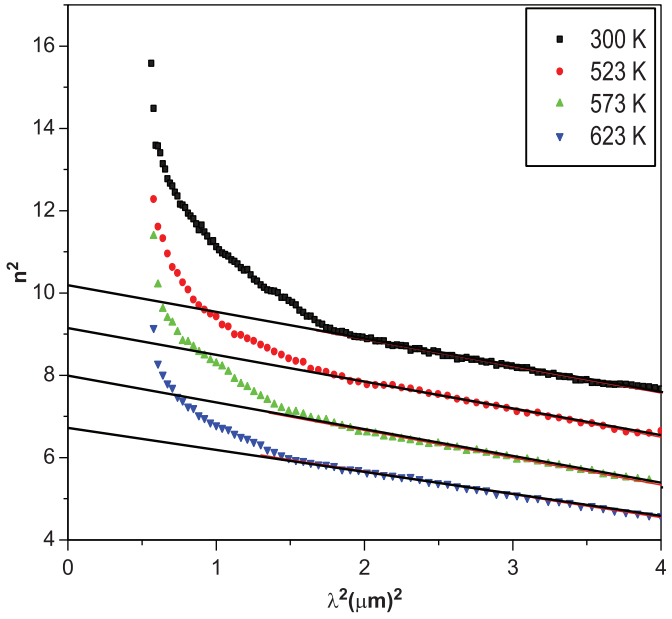

Fig. 15. Plot of n^2 versus λ^2 of $ZnIn_2Se_4$ thin films, with thickness 1254 nm, for as deposited at 300 K and annealed in vacuum at different temperatures.

4. Conclusion

The effect of temperature on $ZnIn_2Se_4$ thin films prepared by the thermal evaporation process with high deposition rate was studied in this paper. $ZnIn_2Se_4$ thin films deposited at room-temperature (300 K) and at substrate temperature of 623 K. The as deposited film of thickness 1254 nm was annealed in vacuum at different temperatures (523, 573 and 623 K). Whereas the formed films at substrate temperature of 623 K were deposited for thickness in the range of 173–346 nm. The room-temperature deposited $ZnIn_2Se_4$ thin films have a nanocrystallite structure with crystallite size of about a few nanometers increased to 31 nm with increasing the annealing temperature up to 623 K. The measurements are performed on the preferred orientation plane (1 1 2). The optical constants of $ZnIn_2Se_4$ thin films were estimated and they were found to be independent on film thickness. The effect of annealing temperature on the optical constants was also investigated. The absorption analysis of the as deposited films revealed the

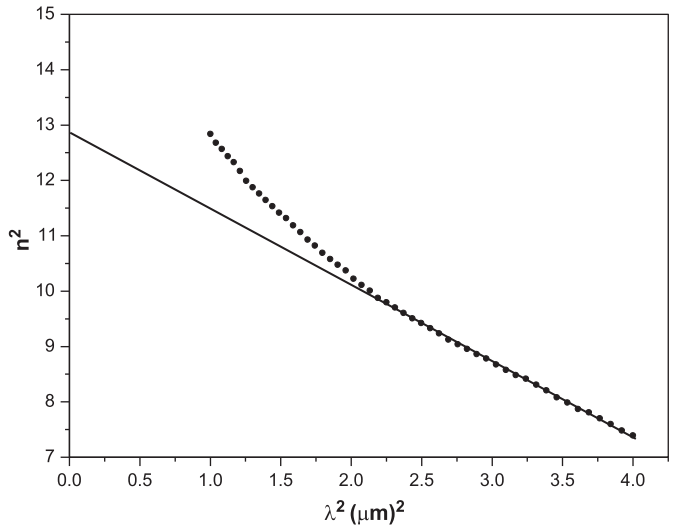

Fig. 16. Plot of n^2 versus λ^2 for as deposited $ZnIn_2Se_4$ thin films at substrate temperature of 623 K.

existence of allowed direct and indirect transitions with optical energy gaps of 2.21 and 1.71 eV respectively. The indirect allowed transition is accompanied with phonon energy of 53 meV. The values of energy gaps decreased with increasing annealing temperature. The direct band gap increased to 2.41 eV for films deposited at substrate temperature of 623 K. The covalent nature of structure was found to decrease with increasing annealing temperatures. The refractive index dispersion data was found to obey the single-oscillator model and the values of the oscillator energy E_o, dispersion energy E_d, dielectric constant at infinite frequency ε_∞, lattice dielectric constant ε_L, nonlinear susceptibility $\chi^{(3)}$ and nonlinear refractive index n_2 were determined as a function of the annealing and substrate temperature.

References

[1] H.P. Trah, V. Krämer, Z. Kristallogr. 173 (1985) 199.
[2] H.M. Zeyada, M.S. Aziz, A.S. Behairy, Physica B 404 (2009) 3957.
[3] J. Luengo, N.V. Joshi, Mater. Lett. 26 (1996) 47.
[4] S. Sgariazzo, A. Serpi, Phys. Rev. B 41 (1990) 7718.
[5] J. Filipowicz, N. Romeo, L. Tarricone, Solid State Commun. 38 (1980) 619.
[6] E. Nowark, B. Neumann, B. Steiner, Phys. Status Solidi A 13 (1992) k13.
[7] E. Fortin, F. Raga, Solid State Commun. 14 (1974) 847.
[8] E. Grilli, M. Guzzi, R. Molteni, Phys. Status Solidi 37 (1976) 399.
[9] R. Trykozko, J. Filipowicz, Jpn. J. Appl. Phys. 119 (1980) 153.
[10] N.M. Mekhtiev, Z.Z. Gruseinov, E.Yu Salaev, Sov. Phys. Semicond. 18 (1984) 677.
[11] G. Doll, A. Anghel, J.R. Baummann, E. Bucher, A.P. Ramirez, K.J. Range, Phys. Status Solidi 1126 (1991) 237.
[12] P. Babu, K.T. Ramakrishna Reddy, R.W. Miles, Energy Procedia 10 (2011) 177.
[13] A.G. Abdullayev, T.G. Kerimova, M.G. Kyazumov, A.S. Khidirov, Thin Solid Films 190 (1990) 309.
[14] C. Paorici, L. Zamotti, G. Zuccalli, J. Cryst. Growth 43 (1980) 705.
[15] S.P. Yadav, P.S. Shinde, K.Y. Rajpure, C.H. Bhosale, J. Phys. Chem. Solids 69 (2008) 1747.
[16] T.A. Hendia, L.I. Soliman, Thin Solid Films 261 (1995) 322.
[17] H.M. Zeyada, M.S. Aziz, A.S. Behairy, Eur. Phys. J. Appl. Phys. 45 (2009) 30601.
[18] A.E. Delahoy, M. Akhtar, J. Cambridge, L. chen, R. Govindarajan, S. Guo, M.J. Romero, Proceedings of 29th IEEE Photovoltaic Specialists Conference, New Orleans, USA, May 19–24, 2002, p. 640.
[19] S. Shionoya, Y. Tamato, J. Phys. Soc. Jpn. 19 (1971) 1142.
[20] L.I. Berger, V.D. Prochukhan, Ternary Diamond Like Semiconductor, Consultants Bureau, New York, London, 1969, p. 85.
[21] J.A. Beun, R. Nitsche, M. Lichtensteiger, Physica 27 (1961) 448.
[22] S.Tolansky, Multiple-Beam Interference Microscopy of Metals, Academic Press, London, 1970, p.55.
[23] M.D. Giulio, G. Micocci, R. Rella, Phys. Status Solidi A 136 (1993) k101.
[24] B.D. Cullity, Elements of X-ray Diffraction, Addison-Wesley, Reading, MA, 1979.
[25] H.J. Fritsche, Non-Cryst. Solids 6 (1971) 49.
[26] A. Bosacchi, B. Bosacchi, S. Franchi, L. Hernandez, Solid State Commun. 23 (1973) 1805.
[27] T.A. Hendia, L.I. Soliman, Thin Solid Films 261 (1995) 322.

[28] H.S. Soliman, M.M. El-Nahass, A. Qusto, J. Mater. Sci. 26 (1991) 1556.
[29] A. Stendal, U. Beckars, S. Wilbrand, O. Stenzel, C. Von Borczys-Kowski, J. Phys. B: At. Mol. Opt. Phys. 29 (1996) 2589.
[30] S.H. Wemple, M. Di Domenico, Phys. Rev. B 3 (1971) 1338.
[31] J. Bardeen, F.J. Slatt, L. Hall, Photoconductivity Conference, Wiley, New York, 1965, p.146.
[32] M. Guzzi, E. Grilli, Mater. Chem. Phys. II (1984) 295.
[33] L.I. Soliman, T.A. Hendia, Radiat. Phys. Chem. 50 (1997) 175.
[34] Kong-Wei Cheng, Ya-Hsin Cheng, Miao-Syuan Fan, Int. J. Hydrogen Energy 37 (2012) 13763.
[35] A. Borghesi, G. Guizzetti, L. Nosenzo, Prog. Cryst. Growth Charact. 13 (1988) 97.
[36] Sung-Hyu Choe, Curr. Appl. Phys. 9 (2009) 1.
[37] G.A. Kumar, J. Thomas, N. George, B.A. Kumar, P.R. Shnan, V.P. Npoori, C.P.G. Vallabhan, N.V. Unnikrishnan, Phys. Chem. Glasses 41 (2001) 31.
[38] M.M. El-Nahass, A.A.M. Farag, E.M. Ibrahim, S. Abd El-Rahman, Vacuum 72 (2004) 453.
[39] J.J. Wyne, Phys. Rev. 178 (1969) 1295.
[40] H. Ticha, L. Tichy, J. Optoelectron. Adv. Mater. 4 (2002) 381.
[41] W.L. Smith, in: M.J. Weber (Ed.), Handbook of Laser Science and Technology, vol. 3, Chemical Rubber Co., Boca Raton, 1986, p. 259, Part 1.